ELSEVIER

Thermochimica Acta 395 (2003) 237–249

thermochimica acta

www.elsevier.com/locate/tca

Thermal transitions of osmotically dehydrated tomato by modulated temperature differential scanning calorimetry

A.F. Baroni[a,*], A.M. Sereno[b], M.D. Hubinger[a]

[a]*Department of Food Engineering, Faculty of Food Engineering, State University of Campinas, 13083-970 Campinas, Brazil*

[b]*CEQUP, Department of Chemical Engineering, Faculty of Engineering, University of Porto, Rua Dr. Roberto Frias, s/n, 4200-465, Porto, Portugal*

Received 26 March 2002; accepted 10 April 2002

Abstract

Modulated temperature differential scanning calorimetry (MTDSC) was employed to examine thermal transitions of osmotically dehydrated tomato (*Lycopersicon esculentum*, var. Deborah). Tomato halves, soaked in sucrose solution (60% sucrose), sodium chloride (10% NaCl) and mixtures of salt–sucrose solution (60% sucrose–10% NaCl/40% sucrose–15% NaCl) for 3 h at 40 °C, were comminuted, freeze-dried for 48 h and kept in desiccator over saturated salt solutions at 25 °C until equilibrium was reached. A MTDSC 2920 (TA Instruments) was used in all tests. A cyclic modulation of ±0.5 °C/40 s was superimposed on a constant scanning ramp of 2.5 °C/min. Thermo-analytical curves of both osmotically dehydrated and untreated tomato allowed the determination of the glass transition data and the plot of state diagrams. Furthermore, a peak of enthalpy relaxation in the glass transition region that partially disappears on rescanning was detected. Structural recovery was modelled by Williams–Watts equation and glass transition temperature by Gordon and Taylor and Kwei equations.

Keywords: Glass transition; Tomato; Enthalpy of relaxation; State diagram; Osmotic treatment

1. Introduction

Glass transitions, their temperature range and magnitude, provide useful information about the structure of the amorphous components of foods. This configuration and its change with time are critical to processing, storage and end-use of a material. Drying of fruits and vegetables induces a progressive concentration of solid matrix presented in protoplasm, resulting in products in glassy state. For pure synthetic polymers, glass transition temperature (T_g) is known to increase with molecular mass with a significant impact on the rheological properties of the material [1]; in spite of a large dispersion of reported data on T_g of pure sugars, values indicated by Roos [2] suggest a similar trend. It would then be expected that an increase on the average molecular mass of the solid matrix of fruits and vegetables may lead to an increase of its glass transition temperature and thus a reduced collapse of final product during drying, for the same process conditions. Osmotic dehydration prior to conventional drying has been presented as a promising method of improving

* Corresponding author. Present address: Department of Chemical and Food Engineering, Faculty of Engineering, Mauá Institute of Technology, Praça Mauá, 1 São Caetano do Sul, Brazil.
E-mail addresses: baroni@maua.br (A.F. Baroni), sereno@fe.up.pt (A.M. Sereno), mhub@ceres.fea.unicamp.br (M.D. Hubinger).

0040-6031/02/$ – see front matter
PII: S0040-6031(02)00220-4

quality of dried food. Higher drying rates were observed when vegetables are pre-treated with salt solutions [3]. The reduction in shrinkage of sugar immersed foods is showed in literature [4–6]. Some authors [7,8] related these improvements to an increase in glass transitions temperatures due to water removal and the impregnation of high molecular substances during osmotic dehydration, consequently lowering temperature difference between glass transition and drying process. State diagrams maps, that show glass transition temperature as a function of water content, can help in the evaluation of osmotic dehydration effect on glass transition temperature, as well as aid in the choice of the best process conditions [9–11].

Very often enthalpy effects are observed during structure relaxation occurring in the glass transition region. This phenomenon results in changes of material properties, such as length, hardness, brittleness, density, creep- and stress-relaxation rates, dielectric constant and dielectric loss [12]. The size of such effects can be used to measure the structural changes. This phenomenon is frequently observed by differential scanning calorimetry (DSC) during heating of a glassy material to a temperature above its glass transition, showing an endothermic peak in glass transition region. A number of glassy food materials have been reported to undergo physical ageing in which a rearrangement of the polymers occurs towards a more energetically stable conformation during storage. However, few events of this kind have been observed for freeze-dried vegetable tissue [13].

Modulated temperature differential scanning calorimetry (MTDSC) is a type of DSC instrument that allows a sinusoidal cycling temperature program to be imposed over the conventional linear heating/cooling ramp. Benefits of MTDSC include the more accurate measurement of heat capacity, the separation of overlapping thermal events and the improved identification of thermal process [14,15]. Especially in the glass transition region where MTDSC is capable of to separating enthalpic relaxation peak from the step change in the heat capacity [16,17]. When conventional DSC is used, the presence of enthalpic relaxation may lead to misinterpreted of the glass transition region as a melting transition. Evaluation of the influence of osmotic dehydration on thermal transitions of freeze-dried tomato by MTDSC was the main purpose of this paper.

2. Experimental

2.1. Tomato

For each experiment test, 40 fresh tomatoes (*Lycopersicon esculentum*, var. Deborah) were purchased at the local market. Twelve tomatoes were selected in order to have homogeneous samples in colour, firmness and around 3.5% (w/w) soluble solids content.

These samples were washed and kept under refrigeration at 4 °C until use. Before tests, tomatoes were washed again, cut into halves and had placenta, columella and seeds removed. The average percent composition, experimentally determined as described by Ranganna [18] is showed in Table 1.

2.2. Osmotic dehydration

Tomatoes halves were soaked in solutions of sucrose (60%, w/w) sodium chloride (10%, w/w) and mixed salt–sucrose solution (60% sucrose–10% NaCl and 40% sucrose–15% NaCl) for 3 h at 40 °C under orbital agitation of 90 rpm. A mass ratio of product to solution of 1:10 was used. After the process, samples were washed with distilled water and gently blotted with an absorbent paper to remove surface moisture. Sugar and salt concentration in immersed samples as well as in fresh ones were determined as described in [18] for tomato products and the water content measured gravimetrically by vacuum oven drying (24 h, 60 °C, 25 mm Hg).

2.3. Sample preparation for thermal analysis

Fresh and osmotically treated tomatoes were crushed, frozen at −18 °C for 24 h, freeze-dried (bench freeze-drier Heto-FD3, Germany, −55 °C, 0.05 bar) for 48 h

Table 1
Average percent composition of tomato var. Deborah

Component	%
Water	93.57 ± 0.73
Ash	0.56 ± 0.05
Fat	0.56 ± 0.10
Protein	0.64 ± 0.06
Carbohydrate	4.63 ± 0.62

Table 2
Total solute content of processed tomatoes

Osmotic solution	Solute content (%, w/w)	
	Sucrose	NaCl
60% sucrose	7.2	–
60% sucrose–10% NaCl	6.9	2.9
40% sucrose–15% NaCl	11.2	6.5
10% NaCl	–	4.6

and kept in desiccator with P_2O_5 until constant weight was reached. These samples were considered ''water-free''. After that, the samples were placed into DSC aluminium pans, weighed and equilibrated over saturated salt solutions in desiccators at 25 °C until equilibrium was reached (Table 2). The final water content was calculated from the mass variation of the samples.

2.4. MTDSC scans

The calorimeter employed was a 2920 Modulated DSC by TA Instruments (New Castle, DE, USA). Tomato samples were hermetically closed in aluminium pans (20 μl) with lids, and the mass of each empty sample pan was matched in advance with the mass of empty reference pan to within ±0.1 mg. For very low temperature experiments (<−70 °C), a liquid nitrogen quench accessory was used; otherwise a mechanical refrigeration system (RCS) was applied. Temperature and melting enthalpy calibrations were performed with indium (mp 156.5 °C; ΔH_m 28.5 J/g, 99.999%, TA Instruments) and water (mp 0.0 °C; ΔH_m 333 J/g, bidistilled and Milli-Q). Dry helium, 25 ml/min, was used as purge gas. Heat capacity calibration was performed with sapphire (99.99%, TA Instruments) and water at the same experimental conditions of tomato samples.

After cooling the sample at 10 °C/min up to −120 °C, measurement of glass transition temperature was carried out on thermo-analytical curves obtained by heating the sample at 2.5 °C/min (period 40 s and amplitude 0.5 °C) until 40 °C was reached. Superimposed over the temperature ramp a sinusoidal modulated signal of adequate amplitude and frequency was used. Modulation frequency and amplitude were selected by the method of Lissajous figures described in [13]. For samples that presented water crystallisation during heating ramp, isothermal annealing was used to determine T'_g [8]. Glass transition temperatures were calculated from deconvoluted reversing signals. Data were treated with Thermal Solutions Software (TA Instruments, New Castle, DE, USA).

For enthalpy relaxation measurements only dry (''water-free'') samples were evaluated. Heating and cooling underlying scanning ramp was 2.5 °C/min (period 40 s and amplitude 0.5 °C), from −20 to 80 °C. The previous history of the samples was erased after heating to 80 °C to obtain the aged thermo-analytical curve. Materials were aged from 10 to 7200 min at 25 °C (∼T_g 15 °C), to correct the frequency effect caused by temperature modulation on MTDSC signals. The non-reversing signal was integrated for both heating and cooling runs and the difference between them was employed [15].

2.5. Plasticising effect on glass transition

Midpoint glass transition temperatures were obtained using TA software and modelled using Couchman theory, simplified here by Gordon and Taylor equation [11]:

$$T_g = \frac{X_s T_{gs} + K X_w T_{gw}}{X_s + K X_w} \quad (1)$$

where X is the mass fraction, T_g the glass transition temperature, K a constant and subscripts s and w refer to solids and water, respectively. K is related to the ratio of the heat capacity increments or volume expansion coefficients of the components. Addition of the term (qX_wX_s) to the Gordon and Taylor equation leads to the Kwei relation:

$$T_g = \frac{X_s T_{gs} + K X_w T_{gw}}{X_s + K X_w} + q X_w X_s \quad (2)$$

where q is a constant and the term (qX_wX_s) seeks to represent the effect of intermolecular forces present in the mixture, such as hydrogen bonding [19].

2.6. Secondary relaxations

The glass–rubber transition is a kinetic process associated with a primary relaxation of the material [20,21]. Secondary relaxation processes are small-scale molecular motions that occur in amorphous glassy state, involving mainly rotations and vibrations

of molecular groups. Craig et al. [22] have recently reviewed this topic in detail.

The extent of the relaxation (ϕ_t) can be calculated at any time and storage temperature as:

$$\phi_t = 1 - \frac{\Delta H_t}{\Delta H_\infty} \quad (3)$$

where ΔH_t is the measured enthalpy of recovery and ΔH_∞ is the corresponding maximum enthalpy, calculated as follows:

$$\Delta H_\infty = (T_g - T_{ag})\Delta C_p \quad (4)$$

where T_g is the glass transition temperature, T_{ag} the ageing temperature and ΔC_p is the heat capacity change during glass transition.

The extent of relaxation (ϕ_t) may be expressed in terms of the mean time of relaxation (τ) and a parameter of relaxation time distribution, β, according to Williams–Watts equation [21,22]:

$$\phi_t = \exp\left(-\frac{t}{\tau}\right)^\beta \quad (5)$$

3. Results and discussion

In order to avoid excessive solute impregnation, likely to affect sensorial characteristics of the material, duration of osmotic treatment was limited. In the experiments, total solute content of tomato samples were as in Table 2. This limited increase in solute content did not produce significant changes of glass transition temperatures; this general behaviour agrees with results reported by Aguilera et al. [6] and Sá et al. [11] for freeze-dried apple.

3.1. Sorption isotherm of osmotic dehydrated samples

The sorption characteristics are very important for the evaluation of the influence of osmotic treatment on glass transition of a material, since water is the most important system plasticiser. For food materials, sorption isotherms showing equilibrium water content versus water activity (ratio of water vapour pressure of the material to the vapour pressure of pure water at the same temperature) are normally used [23,24]. Table 3 shows sorption isotherm data of the samples.

Equilibrium water content of osmotic dehydrated (OD) samples conditioned at high relative humidity is considerably higher than for non-treated samples due to the dissolution of the impregnated solution. Otherwise, at low water activity ($a_w < 0.53$) the equilibrium water content was also low for OD treated samples. Comparing solutes of OD process, one can verify that for samples impregnated with sodium chloride, a more significant raise of equilibrium water content occurs than for only sucrose solution treated pieces, caused

Table 3
Sorption characteristics of the tomato samples

Salt solution	a_w	Equilibrium water content (g water/g dry matter)				
		Untreated	10% NaCl	60% sucrose	60% sucrose–10% NaCl	40% sucrose–15% NaCl
NaOH	0.070	0.039 ± 0.004	0.011 ± 0.001	0.029 ± 0.001	0.029 ± 0.001	0.008 ± 0.000
LiCl	0.113	0.044 ± 0.002	0.017 ± 0.001	0.048 ± 0.003	0.045 ± 0.002	0.017 ± 0.001
CH_3COOK	0.234	0.056 ± 0.001	0.021 ± 0.001	0.083 ± 0.001	0.071 ± 0.002	0.022 ± 0.002
$MgCl_2{\cdot}6H_2O$	0.329	0.082 ± 0.004	0.025 ± 0.001	0.096 ± 0.001	0.089 ± 0.001	0.063 ± 0.002
K_2CO_3	0.443	0.106 ± 0.003	0.060 ± 0.003	0.157 ± 0.003	0.126 ± 0.004	0.112 ± 0.003
$Mg(NO_3)_2$	0.534	0.151 ± 0.002	0.153 ± 0.002	0.223 ± 0.003	0.167 ± 0.003	0.180 ± 0.002
$NaNO_2$	0.611	0.248 ± 0.006	0.518 ± 0.003	0.341 ± 0.005	0.261 ± 0.004	0.420 ± 0.005
NaCl	0.764	0.392 ± 0.002	0.982 ± 0.012	0.762 ± 0.001	0.583 ± 0.006	0.796 ± 0.004
NH_4SO_4	0.810	0.440 ± 0.003	1.140 ± 0.013	0.957 ± 0.021	0.676 ± 0.008	1.072 ± 0.001
KCl	0.846	0.523 ± 0.007	1.509 ± 0.005	1.144 ± 0.005	0.903 ± 0.013	1.303 ± 0.005
K_2CrO_7	0.870	0.778 ± 0.005	1.907 ± 0.027	1.608 ± 0.014	1.090 ± 0.009	1.761 ± 0.021
$BaCl_2{\cdot}2H_2O$	0.902	1.114 ± 0.012	2.561 ± 0.084	1.883 ± 0.006	1.358 ± 0.022	2.281 ± 0.036

Average values of three experimental results and respective standard deviation.

probably by the high hygroscopic behaviour of sodium chloride compared with sucrose.

Several models (empirical, semi-empirical or theoretical) with two or more parameters have been used to describe the water sorption isotherms [26,27]. Equations based in sorption theories are usually preferred by most researches once some physical meaning may be attached to their parameters, helping the understanding of water sorption phenomena. BET model developed the multilayer adsorption concept, very important in estimation of the amount water bound to specific polar sites in dehydrated food systems, nevertheless it was not able to predict water sorption relationships above $a_w = 0.3$ [26]. Modifications in BET equation led to GAB model that has a wide range of applicability (good fit up to $a_w = 0.9$). This equation was recommended by the COST90 project to describe water sorption isotherms of food [28]:

$$X_w = \frac{MCKa_w}{(1 - Ka_w)(1 - Ka_w + CKa_w)} \quad (6)$$

where C and K are constants and M is related to monolayer moisture and a_w the water activity. The parameters obtained as well as the sum of residues are shown in Table 4 where SSE is the sum of squared residues between calculated and experimental data and R^2 the correlation coefficient.

Table 4
GAB parameters for tomato

Sample	M	C	K	SSE	R^2
Untreated	0.073	10.156	1.030	0.026	0.991
40% sucrose–15% NaCl	0.316	0.489	0.988	0.034	0.995
60% sucrose	0.306	0.590	0.969	0.037	0.993
60% sucrose–10% NaCl	0.202	0.816	0.972	0.006	0.998
10% NaCl	0.387	0.427	0.982	0.076	0.992

3.2. Selection of MTDSC experimental conditions

During a MTDSC scan the modulation of the temperature results in a modulated heat-flow. It can be deconvuluted by a discrete Fourier transform algorithm, into reversing and non-reversing heat-flow, for optimum experimental conditions [17]. In glass transition region, the step change in the heat capacity is calculated from the reversing signal while kinetic effects, as enthalpy of relaxation, are observed in the non-reversing signal [14]. Figs. 1 and 2 shows how these two events are separated during the deconvolution of calorimeter signals.

The glass transition is a region that includes both a step change in heat capacity and an enthalpic relaxation peak. The combined heat-flow signal (central line) presents two thermal events that could be easily

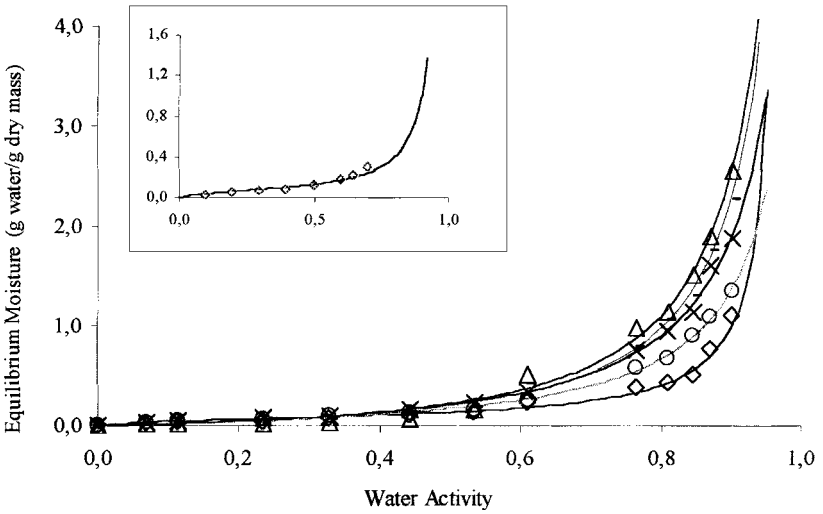

Fig. 1. Water sorption isotherms of OD processed and untreated tomato at 25 °C: (◇) untreated tomato; (▽) 10% NaCl; (×) 60% sucrose; (○) 60% sucrose–10% NaCl; (—) 40% sucrose–15% NaCl (lines represent GAB fitting to data). Inserted plot compares GAB equation fitted to untreated sorption data with data taken from Alcaraz et al. [25] at 27 °C.

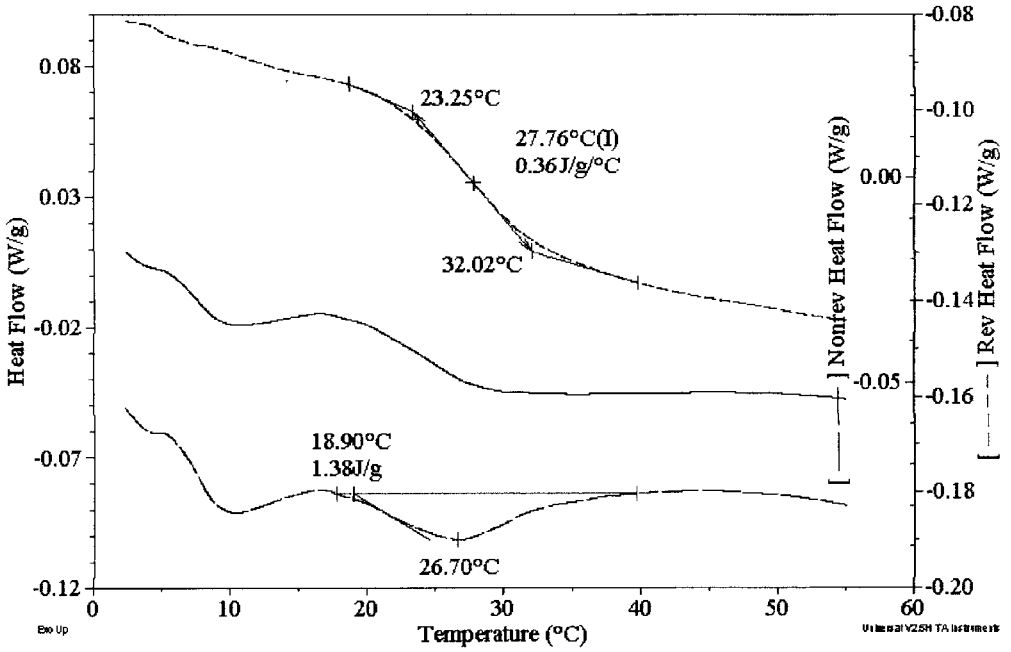

Fig. 2. Glass transition and enthalpy relaxation of dried tomato by MTDSC, $a_w = 0.44$.

interpreted as two glass transitions or the most common sub-T_g endotherm followed by glass transition. MTDSC analysis clears up the events and facilitates its interpretation after deconvolution [16]. A clear glass transition is observed on reversing heat-flow signal while enthalpy relaxation is evident on the curve showing the non-reversing heat-flow signal. However, reliable results are strongly dependent on the choice of modulation parameters and some attention should thus be paid to their selection. The use of Lissajous figures has been proposed to evaluate the quality of sine wave response to a harmonic *stimulus* [14,17]. These figures show when the instrument is in steady state by showing a smooth ellipse. Any distortion indicates the loss of steady state resulting in inaccurate data or even artifact peaks. It is also recommended to have at least five or six cycles of modulation through any transition to enable the deconvolution process performed by instrument software to work properly [17]. Fig. 3 shows Lissajous plots during heating of dried tomato at 2.5 °C/min, 40 s period.

At large amplitudes (1 °C) for a short period (40 s), one can notice that despite an elliptic shape the reproducibility of the cycles is poor (Fig. 3A). Smaller amplitude allows a better heat transfer in and out of the sample at the required modulation, holding the steady state. The use of large periods also favoured elliptical shape of Lissajous plots, however, compromises the requirement of a minimal number of cycles in the range of the thermal transition. The modulation parameters selected (rate 2.5 °C/min, period 40 s and amplitude 0.5 °C) showed to be suitable for all tested samples.

3.3. Thermal behaviour of tomato samples

The observed thermal transitions of osmotically treated and non-treated tomato (Figs. 2 and 4) are similar to those found in other vegetable tissue [6,10–12]. During the heating of a quenched sample a glass transition (reversing heat-flow signal) together with an endothermic undershoot—enthalpy of relaxation (non-reversing heat-flow signal) are observed. The following behaviour is different for low-water content and high water content samples. The latter (Fig. 4) shows an exothermic peak (devitrification, T_d) resulting from crystallisation of freezable water that remained unfrozen within matrix, followed by the melting of ice (T_m) and another exothermic/endothermic event at around 20–50 °C (T_{gel}). A similar event

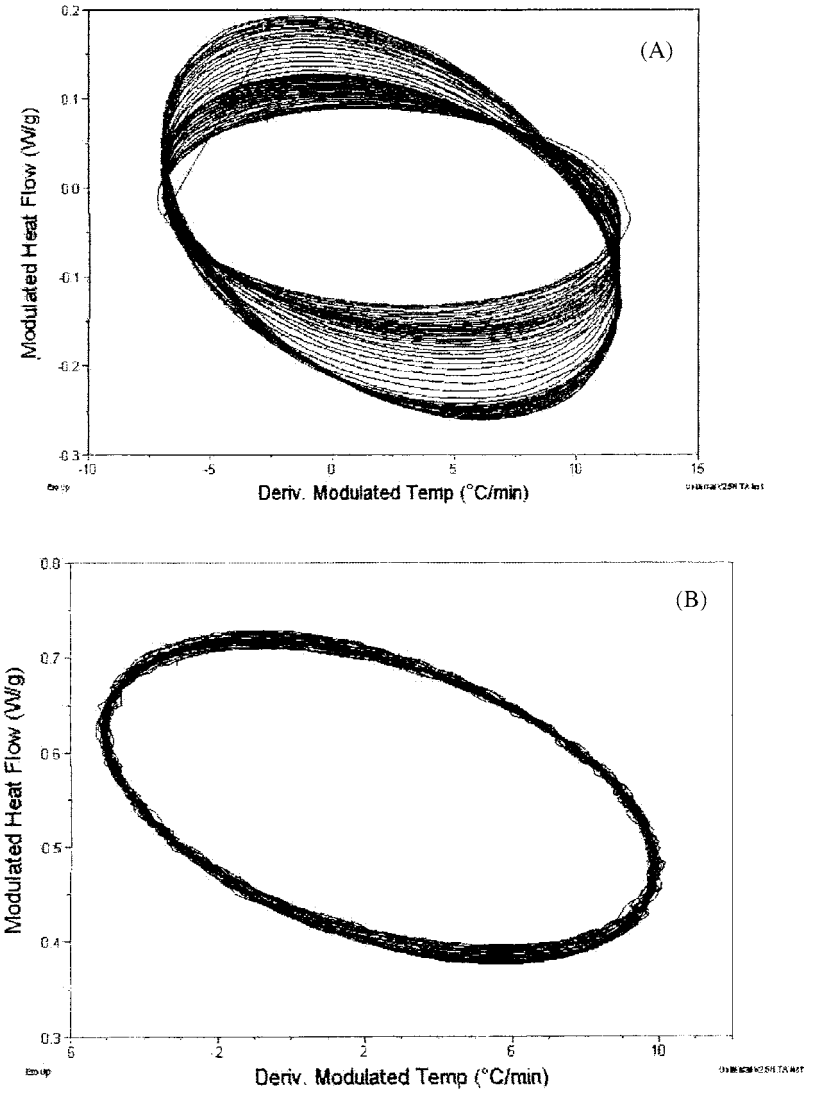

Fig. 3. Lissajous figures obtained during heating of dried tomato from −10 to 60 °C at 2.5 °C/min with 40 s of period: (A) amplitude 1 °C; (B) amplitude 0.5 °C.

was detected by Aguilera et al. [6] on thermo-analytical curves of low-water content apple.

The nature of this endothermic undershoot is unknown, but some hypothesis have been presented. Appelqvist et al. [29] observed similar events for various polysaccharides interpreting them in terms of water–carbohydrate interactions. However, in their study, the endothermic peaks always occurred before glass transition and disappeared on subsequent rescans. In tomato thermo-analytical curves, the endothermic peaks show up clearly after glass transition and melting of ice and reappear in the same way on rescanning; a possible explanation is that this event is due to gelatinisation of tomato pectin (T_{gel}), which is thermally reversible [30,31].

3.4. Glass transition

Fig. 5 presents typical glass transitions of untreated tomato for samples that did not present devitrification

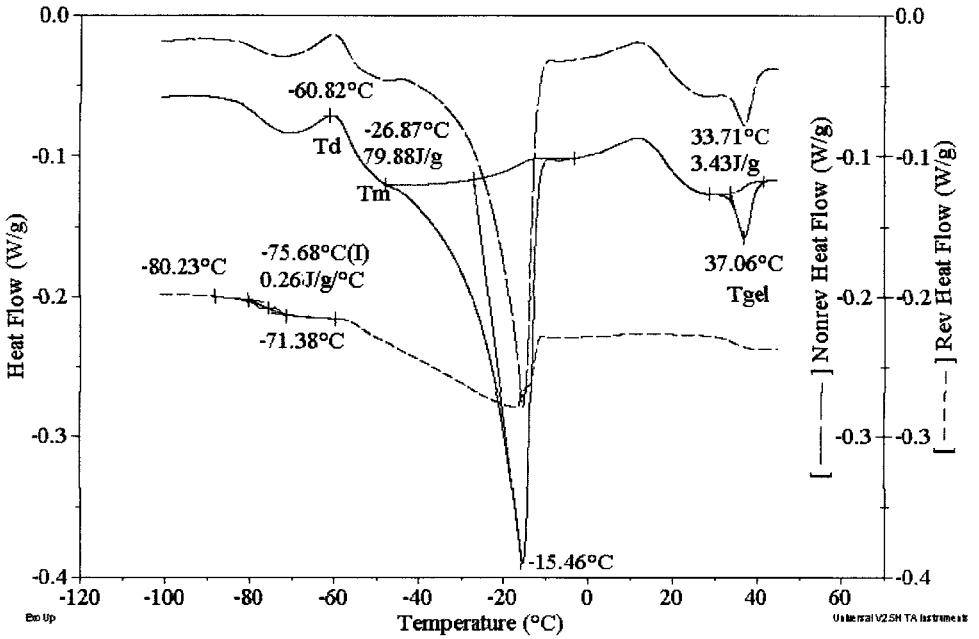

Fig. 4. Thermal transitions of osmotic dehydrated tomato (40% sucrose–15% NaCl), $a_w = 0.87$.

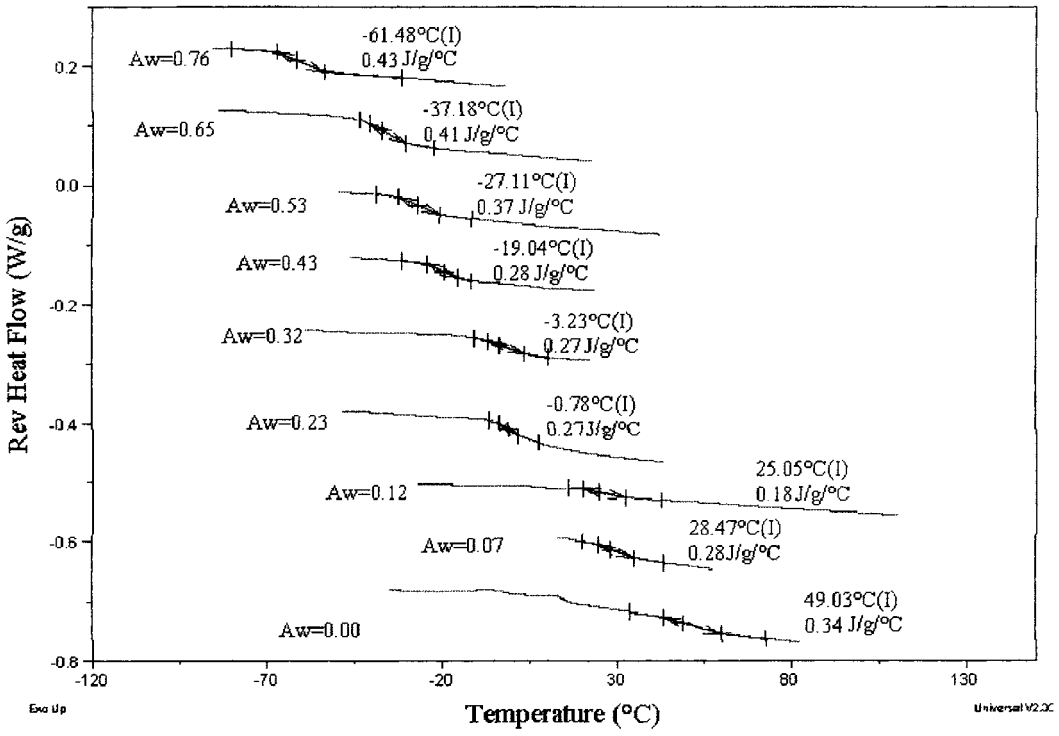

Fig. 5. Midpoint glass transition temperature and transition ΔC_p of untreated tomato. Baselines adjusted to produce the stacking effect.

Table 5
Midpoint glass transition temperature (T_{gm}) and ΔC_p of tomato

a_w	Untreated		60% sucrose	
	T_{gm} (°C)	ΔC_p (J/g K)	T_{gm} (°C)	ΔC_p (J/g K)
0.00	49.05 ± 0.03	0.32 ± 0.03	43.20 ± 0.07	0.41 ± 0.02
0.070	28.39 ± 0.12	0.23 ± 0.05	4.98 ± 0.05	0.30 ± 0.03
0.113	26.50 ± 0.10	0.18 ± 0.00	2.74 ± 0.64	0.23 ± 0.03
0.234	−0.79 ± 0.01	0.30 ± 0.04	0.89 ± 0.62	0.26 ± 0.02
0.329	−3.23 ± 0.01	0.31 ± 0.05	−9.48 ± 1.10	0.22 ± 0.02
0.443	−18.27 ± 1.09	0.32 ± 0.05	−21.03 ± 0.84	0.29 ± 0.02
0.534	−27.94 ± 1.17	0.39 ± 0.02	−31.80 ± 0.16	0.27 ± 0.00
0.611	−37.20 ± 0.02	0.43 ± 0.03	−48.62 ± 0.47	0.33 ± 0.00
0.764	−60.87 ± 0.87	0.45 ± 0.03	−67.29 ± 0.60	0.32 ± 0.04

Average values of three experimental results and respective standard deviation.

peaks. All samples followed a similar behaviour as shown in Fig. 5. The increase of water activity led to a lower glass transition temperature due to the plasticising effect of water [2,10]. As ΔC_p is related to the molecular mobility during glass transition, samples with greater water content presented high values for ΔC_p. However, ΔC_p is also related to the level of aggregation/reorganisation of the molecules; the high values for ΔC_p observed for nearly "water-free" samples mean that they are probably vitrified with greater molecular disorder than the other ones [32].

Tables 5 and 6 show average midpoint glass transition temperature and respective ΔC_p of samples not presenting a devitrification peak. One can notice slightly high values of ΔC_p for osmotic dehydrated samples, especially in solutions having sodium chloride, compared with untreated ones. As has been described, these samples presented a high equilibrium water content up to $a_w = 0.53$, therefore by the presence of water, more molecular mobility is found in this case.

3.5. State diagram

Two different thermodynamic models (Gordon and Taylor and Kwei) were fitted to experimental data in order to describe the plasticising effect on macromolecules of tomato solid matrix. Table 7 shows experimental T'_g and the calculated empirical parameters. Data and model curves are plotted in Fig. 6 for untreated tomato and after treatment with 40% sucrose–15% NaCl solution for 3 h.

A reduction of T_g in osmotic treated samples was observed. This behaviour may be explained by the impregnation of the solid matrix with a solute of lower molecular weight. In the case of tomato treated with pure sucrose solution, T_g values obtained moved slightly towards T_g values of pure sucrose at the same

Table 6
Midpoint glass transition temperature (T_{gm}) and ΔC_p of tomato

a_w	40% sucrose–15% NaCl		60% sucrose–10% NaCl		10% NaCl	
	T_{gm} (°C)	ΔC_p (J/g K)	T_{gm} (°C)	ΔC_p (J/g K)	T_{gm} (°C)	ΔC_p (J/g K)
0.00	28.08 ± 0.54	0.38 ± 0.01	33.69 ± 0.21	0.51 ± 0.01	35.27 ± 0.01	0.46 ± 0.03
0.070	26.40 ± 0.03	0.87 ± 0.03	13.65 ± 1.48	0.52 ± 0.04	27.59 ± 2.09	0.48 ± 0.08
0.113	13.76 ± 0.08	0.24 ± 0.01	7.47 ± 0.16	0.50 ± 0.01	−0.23 ± 1.94	0.49 ± 0.04
0.234	1.23 ± 1.77	0.32 ± 0.05	−10.41 ± 1.20	0.45 ± 0.02	−8.27 ± 0.31	0.50 ± 0.03
0.329	−16.23 ± 0.58	0.35 ± 0.02	−14.76 ± 0.71	0.26 ± 0.01	−8.71 ± 0.87	0.51 ± 0.01
0.443	−33.17 ± 0.45	0.38 ± 0.01	−33.39 ± 0.28	0.49 ± 0.05	−28.03 ± 1.28	0.50 ± 0.04
0.534	−51.07 ± 0.44	0.51 ± 0.04	−50.64 ± 0.56	0.61 ± 0.01	−50.22 ± 0.59	0.50 ± 0.05
0.611	−75.06 ± 0.52	0.70 ± 0.09	−73.48 ± 0.88	0.73 ± 0.03	−80.23 ± 0.91	0.78 ± 0.04

Average values of three experimental results and respective standard deviation.

Table 7
Data of state diagram of tomato and parameters of Eqs. (1) and (2)

Sample	Experimental data	Gordon and Taylor		Kwei		
	T'_g (°C)	K_g	R^2	K_k	q	R^2
Untreated	−50.21 ± 0.47	3.33	0.98	3.84	43.03	0.98
60% sucrose	−49.22 ± 0.38	3.54	0.99	5.10	104.6	0.99
60% sucrose–10% NaCl	−53.31 ± 1.07	5.54	0.99	6.58	163.8	0.99
40% sucrose–15% NaCl	−57.31 ± 1.21	5.35	0.99	10.2	166.5	0.99
10% NaCl	−55.15 ± 0.87	7.32	0.96	18.2	195.3	0.99

Average values of three experimental results and respective standard deviation.

water content. When sodium chloride was added to the solution, a larger decrease of T_g was observed; the lowest T_g values at constant water content were obtained with pure sodium chloride. This behaviour is clearly presented in Table 8.

Measured values of glass transition temperature of the concentrated amorphous solution (T'_g) were similar to those presented by Telis and Sobral [33] for pineapple, −51.6 °C; Sá [34] for freeze-dried grapes, −55.1 °C, and strawberries, −55.8 °C and were slightly affected by osmotic treatment. Lower values were measured for salted samples, probably because of the low molecular weight of sodium chloride compared with sucrose.

Analysing the fitted models, high values of K for samples treated with brine solutions can be noticed. Since K is related to the plasticising effect of water, it suggests that the presence of sodium chloride within the vegetable tissue increases this plasticising effect. These results are consolidated by the q parameter in Kwei equation. According to Georget et al. [13], $q > 0$ indicates the presence of strong interactions between water and cell wall polymers. The addition of sucrose leads only to a slightly T_g change, in spite of a q value twice than for non-treated tomatoes. The addition of salt has apparently increased such interaction (larger q values) with the solid matrix with a consequent decrease in T_g. These results agree with the general

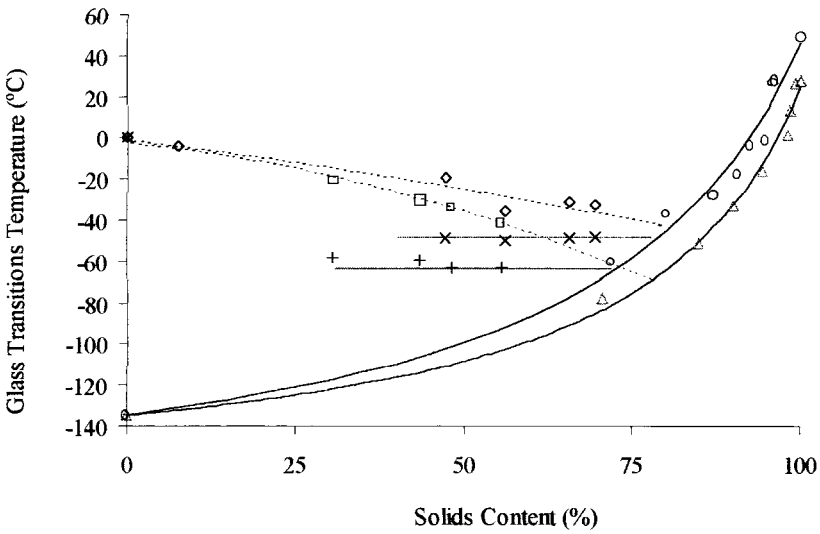

Fig. 6. State diagram for untreated (U) and osmotic dehydrated (OD) tomato: (△) T_g (OD); (○) T_g (U); (□) T_m (OD); (◇) T_m (U); (×) T'_g (OD); (+) T'_g (U); (—) Gordon and Taylor model.

Table 8
Glass transition temperatures (°C) of pure sucrose [2] and osmotic treated tomato

Sample	Water content (%)		
	10	20	40
Untreated	−10.2	−45.3	−86.3
60% sucrose	−10.6	−44.6	−85.4
Pure sucrose [6]	−18.3	−55.6	−94.4
60% sucrose–10% NaCl	−30.6	−64.3	−99.0
40% sucrose–15% NaCl	−32.1	−64.0	−98.1
10% NaCl	−41.0	−74.8	−120.8

mechanism of plasticisation proposed by Matveev et al [35].

3.6. Enthalpy of relaxation

The frequency of the temperature cycling affects heat capacity and reversing signals, shifting the temperature such as in Dynamical Mechanical Analysis (DMA) and Dynamical Electrical Analysis (DEA) experiments. Since non-reversing signal is calculated from heat capacity measurements, corrections for this "frequency effect" must be done by subtracting the area obtained during cooling from the area obtained on heating [15].

Fig. 7 shows a thermo-analytical curve of dried tomato treated in 40% sucrose–15% NaCl solution annealed for 48 h at 25 °C. It has been shown that for some food components such as sucrose, maltose and starch [36,37], the enthalpy of relaxation is not a linear process, due to the presence of shorter and longer relaxation time components. Not even a simple exponential kinetics as proposed by Petrie–Marshal (Eq. (5) with $\beta = 1$) proved acceptable. Williams–Watts model accounts for a non-exponential function of the extension of relaxation (ϕ) and has given fairly good fit for many relaxation processes in a large variety of amorphous materials [37]. Table 9 presents values of parameters fitted to Williams–Watts model.

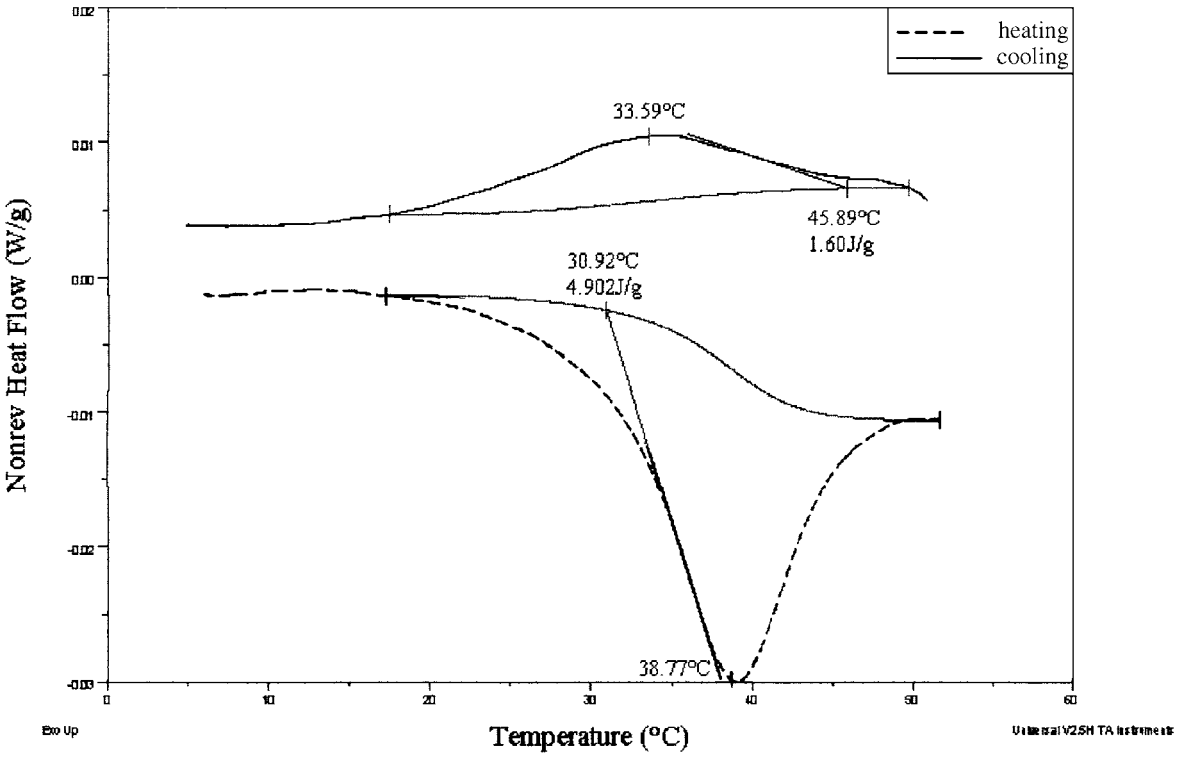

Fig. 7. Thermo-analytical curve of enthalpy of relaxation of OD tomato.

Table 9
Parameters of Eq. (5)

Sample	Williams–Watts model		
	τ (h)	β	R^2
Untreated	407.6	0.579	0.99
60% sucrose	286.29	0.598	0.89
60% sucrose–10% NaCl	326.75	0.564	0.99
10% NaCl	299.73	0.515	0.98
40% sucrose–15% NaCl	312.5	0.531	0.98

High relaxation times (τ) were obtained compared with single food components such as sucrose ($\tau = 20$ h [15]), probably due to the presence of macromolecules and the complexity of bonding in the food solid matrix. However, some differences were observed among the samples; lower τ values were obtained for osmotic treated samples, indicating a high molecular mobility of glass matrix towards equilibrium; on the other hand, β values were quite similar for all cases and slightly higher than those found for sucrose ($\beta = 0.38$ [14]; $\beta = 0.32$ [31]). According to Noel et al. [36], the physical significance of these parameters is difficult to assess and comparison of obtained results is complicated due to the differences in fitting methods, measurement protocols and material variations.

4. Conclusions

Osmotic treatments affected sorption characteristics of untreated tomato, increasing equilibrium water content of samples for $a_w > 0.53$. Similarly, glass transition temperatures of processed pieces were affected by the osmotic treatment, particularly in the presence of sodium chloride that led to a depression on T_g. Upon annealing, devitrified samples were obtained that consistently produced a glass transition temperature corresponding to a maximally freeze-concentrated solid matrix, T'_g.

The use of Lissajous figures allowed the selection of adequate modulation parameters for all tested samples. MTDSC was able to separate glass transition (reversing heat-flow) and enthalpy of relaxation (non-reversing heat-flow). Empirical K parameter for Gordon and Taylor as well as for Kwei equation was higher for osmotically dehydrated tomato than for untreated ones. Times of relaxation calculated from Williams–Watts model were quite similar for all studied samples, however, higher than published sucrose studies.

Acknowledgements

The authors are grateful to FAPESP, CNPq-ICCTI International Co-operation Project, CNPq (No. 300441/886) and to Cyted-Project XI.12.

References

[1] L. Slade, H. Levine, Crit. Rev. Food Sci. Nutr. 30 (1991) 115–360.
[2] Y.H. Roos, Phase Transition in Foods, Academic Press, London, 1995, p. 115.
[3] A.F. Baroni, M.D. Hubinger, Drying Tech. 16 (1998) 2083.
[4] A.F. Baroni, M.D. Hubinger, in: Proceedings of the 12th International Drying Symposium, IDS2000, Elsevier, Amsterdam, 2000.
[5] A. Nieto, D. Salvatori, M.A. Castro, S.M. Alzamora, J. Food Eng. 36 (1998) 63.
[6] J.M. Aguilera, T.R. Cuadros, J.M. del Valle, Carbohydr. Polym. 37 (1998) 79.
[7] S.A. Anglea, Structural Collapse During Dehydration of Plant Tissues and Model System, PhD Thesis, Rutgers University, NJ, USA, 1994.
[8] Y.H. Roos, Phase Transition in Foods, Academic Press, London, 1995.
[9] F. Franks, M.H. Asquith, C.C. Hammond, H.B. Skaer, J. Echlin, J. Microb. 110 (1977) 223.
[10] M.M. Sá, A.M. Sereno, Thermochim. Acta 246 (1994) 285.
[11] M.M. Sá, A.M. Figueredo, A.M. Sereno, Thermochim. Acta 329 (1999) 31.
[12] A.M. Lammert, S.J. Schmidt, in: Proceedings of the ISOPOW 7, Helsinki, Finland, 1998, p. 47.
[13] D.M.R. Georget, A.C. Smith, K.W. Waldron, Thermochim. Acta 332 (1999) 203.
[14] A. Boller, Y. Jin, B. Wunderlich, J. Therm. Anal. 42 (1994) 307.
[15] S. Aubuchon, in: Proceedings of the 2nd Annual NATAS follow up Seminar, TA Instruments, 1998, p. 1.
[16] N.J. Coleman, D.Q.M. Craig, Int. J. Pharm. 135 (1996) 13–29.
[17] V.L. Hill, D.Q.M. Craig, L.C. Feely, Int. J. Pharm. 161 (1998) 95.
[18] S. Ranganna, Handbook of Analysis and Quality Control for Fruit and Vegetable Products, Tata McGraw-Hill, New Delhi, 1986.
[19] T.K. Kwei, J. Polym. Sci., Part C, Polym. Lett. 22 (1984) 307.

[20] D. Champion, M. Le Meste, D. Simatos, Trends Food Sci. Tech. 11 (2000) 41.
[21] K. Six, G. Verreck, J. Peeters, P. Augustijns, R. Kinget, G. Van den Mooter, Int. J. Pharm. 213 (2001) 163–173.
[22] D.Q.M. Craig, P.G. Royall, V.L. Kett, M.L. Hopton, Int. J. Pharm. 79 (1999) 179.
[23] T.P. Labuza, Food Technol. 22 (1968) 263.
[24] M. Loncin, J.J. Bimbenet, L. Lengues, Food Technol. 3 (1968) 131.
[25] E.C. Alcaraz, M.A. Martín, J.P. Marín, Grasas y Aceites 28 (1977) 403.
[26] C. Van den Berg, S. Bruin, in: L.V. Rockland, G.F. Stuart (Eds.), Water Activity: Influences on Food Quality, Academic Press, New York, 1981.
[27] S. Rahman, Food Properties Handbook, CRC Press, New York, 1995.
[28] W.E. Spiess, W.R. Wolf, in: R. Jowitt, F. Escher, B. Hallstrom, H. Meffert, W. Spiess, G. Vos (Eds.), Physical Properties of Foods, Elsevier, London, 1987, p. 65.
[29] I.A.M. Appelqvist, D. Cooke, M.J. Gidley, S.J. Lane, Carbohydr. Polym. 20 (1993) 291.
[30] P.M. Gilsenan, R.K. Richardson, E.R. Morris, Carbohydr. Polym. 41 (2000) 339.
[31] V. Evangeliou, R.K. Richarson, E.R. Morris, Carbohydr. Polym. 42 (2000) 245.
[32] V. Micard, S. Guilbert, Int. J. Biol. Macromol. 27 (2000) 229.
[33] V.R.N. Telis, P.J.A. Sobral, Lebensm. Wiss. U. Tecnol. 34 (2001) 199.
[34] M.M. Sá, Interpretação e do comportamento e estabilidade dos alimentos, PhD Thesis, Faculty of Engineering, University of Porto, Porto, Portugal, 1997.
[35] Y.I. Matveev, V.Y. Grinberg, V.B. Tolstoguzov, Food Hydrocol. 14 (2000) 425.
[36] T.R. Noel, R. Parker, S.M. Ring, S.G. Ring, Carbohydr. Res. 319 (1999) 166.
[37] R. Urbani, F. Sussich, S. Prejac, A. Cesàro, Thermochim. Acta 340 (1997) 359.